# The core of the bacterial translocase harbors a tilted transmembrane segment 3 of SecE

Veenendaal, A.K.J.; van der Does, C.; Driessen, A.J.M.

*Published in:*
The Journal of Biological Chemistry

*DOI:*
10.1074/jbc.M205713200



*Publication date:*
2002

THE JOURNAL OF BIOLOGICAL CHEMISTRY
Vol. 277, No. 39, Issue of September 27, pp. 36640–36645, 2002
Printed in U.S.A.


# The Core of the Bacterial Translocase Harbors a Tilted Transmembrane Segment 3 of SecE*

Received for publication, June 10, 2002, and in revised form, July 12, 2002
Published, JBC Papers in Press, July 22, 2002, DOI 10.1074/jbc.M205713200

**Andreas K. J. Veenendaal, Chris van der Does, and Arnold J. M. Driessen‡**

*From the Department of Microbiology, Groningen Biomolecular Sciences and Biotechnology Institute, University of Groningen, Kerklaan 30, 9751 NN Haren, The Netherlands*

**The bacterial translocase mediates the translocation and membrane integration of proteins. The integral membrane proteins SecY and SecE are conserved core subunits of the translocase. Previous cysteine-scanning studies showed that the transmembrane segment (TMS) 3 of SecE contacts TMS 2 and 7 of SecY, and TMS 3 of another SecE. We now demonstrate that SecE also contacts TMS 10 of SecY. Combining all available cysteine-scanning mutagenesis data, a three-dimensional model has been built in which the positions of the helices that form the central core of the bacterial translocase are mapped. Remarkably, this model reveals that TMS 3 of SecE is strongly tilted relative to SecY.**

In bacteria, the translocase mediates the translocation of proteins across and integration of membrane proteins into the cytoplasmic membrane. Translocase consists of the membrane-bound SecA and the integral membrane protein complex SecYEG (for reviews see Refs. 1 and 2). SecY, SecE, and SecG are membrane proteins that together form a heterotrimeric complex (3, 4), which constitutes a high affinity binding site for SecA (5). SecA is a large dimeric ATPase and drives the stepwise translocation of precursor proteins (preproteins) across the membrane by cycles of ATP binding and hydrolysis (6–8). SecYEG can associate with another trimeric complex consisting of SecD, SecF, and YajC that is required for efficient protein export *in vivo* (9).

SecY and SecE are essential subunits of the translocase. SecY harbors 10 transmembrane segments (TMSs)[1] (see Fig. 1), whereas SecE has a single TMS in most bacteria. In *Escherichia coli*, SecE contains three TMSs (see Fig. 1), but only the conserved C-terminal domain including the third TMS is essential for a functional translocase (10). SecY forms a stable complex in the membrane with SecE that does not dissociate *in vivo* (11) and is rapidly degraded by FtsH when uncomplexed (12). Several domains of SecY and SecE have been suggested to be in close contact. Mutations in the fourth cytoplasmic loop (C4) of SecY (13) and C2 and TMS 3 of SecE (14) destabilize the SecYE complex. Furthermore, specific combinations of *prlA* (SecY) and *prlG* (SecE) mutations result in synthetic lethality (15). Prl (for protein localization) is a class of mutants that suppresses signal sequence defects, and the synthetic lethality has been suggested to signify interactions between periplasmic loop 1 (P1) of SecY and P2 of SecE and TMS 7 and 10 of SecY and TMS 3 of SecE (15). Indeed, cysteine-directed cross-linking studies demonstrated contacts between P1 of SecY and P2 of SecE (16) and between TMS 3 of SecE and TMS 2 (17) and 7 (18) of SecY. Most of the conserved residues and *prlA* mutations are clustered in TMS 2, 7, and 10 of SecY. Furthermore, TMS 2 and 7 of Sec61$\alpha$, the yeast homologue of SecY, have been implicated in the binding of the signal sequence of the preprotein (19). These data strongly suggest a conserved core of the translocase, consisting of TMS 2, 7, and 10 of SecY and TMS 3 of SecE that is involved in preprotein binding.

The SecYEG protomer is a dynamic complex that can organize into dimers and tetramers as revealed by electron microscopy, cysteine-scanning mutagenesis, sedimentation analysis, and Blue Native (BN)-PAGE (18, 20–22). An activated state of the SecA dimer (*i.e.* with a non-hydrolyzable ATP analog or with a trapped preprotein intermediate) was found to be associated with large ringlike SecYEG oligomers that could be fitted to the size of a SecYEG tetramer (20). BN-PAGE demonstrates that a trapped preprotein intermediate remains stably associated with SecYEG dimers in the absence of SecA (22). A chemical cross-linking study failed to demonstrate the presence of SecYEG oligomers, and it was suggested that such forms represent aggregates formed as an artifact of the overproduction (23). However, cysteine-directed cross-linking demonstrates that TMS 3 of SecE contacts a neighboring SecE molecule (17, 18) within a dimeric SecYEG assembly even when present at wild-type levels of the translocase (18), whereas BN-PAGE indicates that the chemical cross-linking interferes with the oligomerization of SecYEG (22). The exact number of SecYEG subunits within the active oligomeric translocase complex, however, is a topic of discussion.

A central question is how the SecYEG complex forms the protein-conducting channel. To answer this, detailed information is required about the molecular architecture of the SecYEG complex. For this purpose, we have initiated a cysteine-scanning mutagenesis approach to probe sites of interaction between SecY and SecE (17, 18). A model has been presented in which one face of TMS 3 of SecE stably interacts with TMS 2 and 7 of SecY whereas the opposite face dynamically interacts with TMS 3 of a neighboring SecE molecule that is part of a separate SecYEG complex. The periodic reappearance of the contacts suggests the presence of $\alpha$-helices as the secondary structure of the investigated transmembrane segments. Based on the conserved residues and the high incidence of *prlA* mutations in TMS 10 and observed synthetic lethal combinations of *prlA* and *prlG* mutations, we expected also that TMS 10 of SecY is located in the core of the translocase in close vicinity to SecE. Here, we indeed present evidence that TMS 3 of SecE contacts TMS 10 of SecY periodically in space. Using our com-

* This work was supported by the Council for Chemical Sciences of the Netherlands Organization for Scientific Research (CW-NWO) and subsidized by the Dutch Organization for the Advancement of Scientific Research (NWO). The costs of publication of this article were defrayed in part by the payment of page charges. This article must therefore be hereby marked "*advertisement*" in accordance with 18 U.S.C. Section 1734 solely to indicate this fact.

‡ To whom correspondence should be addressed. Tel.: 31-503632164; Fax: 31-503632154; E-mail: a.j.m.driessen@biol.rug.nl.

[1] The abbreviations used are: TMS, transmembrane segment; BN, Blue Native; IMV, inner membrane vesicle.

TABLE I
*Plasmids*

Plasmids containing an isopropyl-β-D-thiogalactoside-inducible *trc* promotor before a synthetic *secYEG* operon were used for the overexpression of the Sec YEG complex.

| Plasmid | Relevant characteristic | Mutation | Source |
|---|---|---|---|
| pET607 | Cysteine-less SecYEG in pET610 | C329S (TGT→AGT); C385S (TGC→AGC) | Ref. 17 |
| | SecY TMS 10 mutants in pET607: | | |
| pET2510 | L406C | L406C (CTG→TGT) | This work |
| pET2511 | L407C | L407C (CTT→TGT) | This work |
| pET2512 | I408C | I408C (ATC→TGT) | This work |
| pET2513 | V409C | V409C (GTT→TGT) | This work |
| pET2514 | V410C | V410C (GTT→TGT) | This work |
| pET2515 | V411C | V411C (GTC→TGT) | This work |
| pET2516 | V412C | V412C (GTG→TGT) | This work |
| pET2517 | I413C | I413C (ATT→TGT) | This work |
| | SecE TMS 3 mutants in pET607: | | |
| pET2500 | L95C | L95C (CTG→TGT)[a] | Ref. 18 |
| pET2501 | I96C | I96C (ATT→TGT)[a] | Ref. 18 |
| pET2502 | V97C | V97C (GTG→TGT)[a] | Ref. 18 |
| pET2503 | A98C | A98C (GCT→TGT)[a] | Ref. 18 |
| pET2504 | A99C | A99C (GCG→TGT)[a] | Ref. 18 |
| pET2521 | V100C | V100C (GTT→TGT)[a] | Ref. 18 |
| pET2522 | T101C | T101C (ACC→TGC)[a] | Ref. 18 |

[a] Δ*ClaI* (ATCGAT→ATCGAC) between the *SecY* and *SecE* gene. The names of the double cysteine mutants are combined, *e.g.* pET2513/2522 contains SecY V409C and SecE T101C mutations.

bined data, a three-dimensional model is presented that compiles all the identified contacts in the membrane between SecY and SecE. This model reveals that TMS 3 of SecE is at the contact interface between two SecYEG protomers and must be strongly tilted to accommodate the various observed interactions.

## EXPERIMENTAL PROCEDURES

*Materials*—SecA (24), SecB (25), and proOmpA (26) were purified as described. A stock solution of 80 mM $Cu^{2+}(phenanthroline)_3$ (Sigma) was prepared as described previously (17).

*Plasmids*—The plasmids used to overproduce SecYEG are listed in Table I. Single cysteine mutations in TMS 10 were introduced by a two-step polymerase chain reaction using plasmid pET607 (that allows overexpression of a cysteine-less SecYEG with an N-terminal $His_6$ tag on SecY) as the template (17). Combining cysteine mutations in TMS 10 of SecY and TMS 3 of SecE was accompanied by the deletion of a *Cla*I site between SecY and SecE to facilitate the screening for correct mutants (17). All mutations were confirmed by complete sequence analysis.

*Bacterial Strains, Growth Conditions, and Membrane Vesicle Preparation*—Cell growth and isolation of inner membrane vesicles (IMVs) were performed as described previously (17).

*Cross-linking*—For assays of disulfide bridge formation, IMVs (1 mg/ml) were oxidized with 1 mM $Cu^{2+}(phenanthroline)_3$ for 30 min at 37 °C. The oxidation reaction was quenched by the addition of 25 mM neocuproine (Sigma). Samples were analyzed by 12% SDS-PAGE, Western blotting onto polyvinylidene difluoride membranes (Amersham Biosciences), and immunostaining using antibodies directed against SecY or SecE (27).

*Three-dimensional Modeling*—The stretches of amino acids representing TMS 2, 7, and 10 of SecY and TMS 3 of SecE were constructed as α-helices with the HyperChem (Hypercube Inc.) software, exported in the Brookhaven PDB file format, and subsequently visualized with Weblab Viewer (Accelrys Inc.). The sites of contact between SecE and SecY and a neighboring SecE were highlighted, and a model was built by fitting the matching sites in the best possible way.

*Miscellaneous Methods*—Translocation reactions were essentially performed as described (17) with the difference that the radioactive label ($^{125}I$) on proOmpA was replaced by a fluorescent label (fluorescein maleimide), and translocated proOmpA was visualized with a Lumi-Imager F1 (Roche, Basel, Switzerland).[2] Protein concentrations were determined with the *DC* protein assay (Bio-Rad) using bovine serum albumin as a standard.

[2] J. de Keyzer, C. van der Does, and A. J. M. Driessen, submitted for publication.

## RESULTS

*Construction, Expression, and Activity of Single Cysteine Mutants of SecY*—Unique cysteine mutations were introduced into TMS 10 of SecY to investigate possible contacts with TMS 3 of SecE as suggested by the synthetic lethality of combined *prlA* and *prlG* mutants (15). The previously constructed SecE mutants (L95C to T101C) (18) were located at the cytosolic side of TMS 3. The new set of eight consecutive mutations (L406C to I413C) of SecY covers at least two turns of the putative α-helical structure of TMS 10. Sequence alignment and hydrophobicity analysis predict the same depth in the membrane as for the SecE mutants (Fig. 1). The single cysteine SecY mutations were placed into a cysteine-less SecYEG expression vector (17), and the mutant SecYEG complexes were overproduced in *E. coli* strain SF100. IMVs derived from these cells were analyzed for the SecY and SecE expression levels and proOmpA translocation activity. The *in vitro* translocation assay monitoring the protease protection of the translocated proOmpA was performed as described (17) except that fluorescein maleimide-proOmpA was used instead of $^{125}I$-proOmpA,[2] and visualization of the fluorescent bands in the gel after SDS-PAGE was done with a fluorescence imager. Cysteine-less SecYEG was used as the control because it is indistinguishable from wild-type SecYEG (17). The expression level of the SecYEG mutants as analyzed by SDS-PAGE and Coomassie Brilliant Blue staining were found to be similar to that of the overexpressed cysteine-less SecYEG complex with one exception. IMVs harboring mutant SecY(I408C)EG showed a lower expression of SecY but not of SecE (data not shown) and a correspondingly lower translocation activity (Fig. 2). Fig. 2 suggests a slightly lower activity for mutant Y(V411C)EG. However, this is not representative for SecY(V411C)EG as repeated experiments show a translocation activity for the mutant that is similar to wild-type SecYEG (data not shown). The cysteine mutations did not produce a strong *prl* phenotype as none of the mutants supported the translocation of Δ8-proOmpA, a preprotein with a defective signal sequence that is translocated by PrlA4 (Refs. 28 and 29 and data not shown), nor did they reveal a significantly higher proOmpA translocation activity (Fig. 2).

*TMS 10 of SecY Contacts TMS 3 of SecE at an α-Helical Interface*—To identify possible sites of contact between SecY and SecE, 56 pairs of cysteine mutations were constructed of

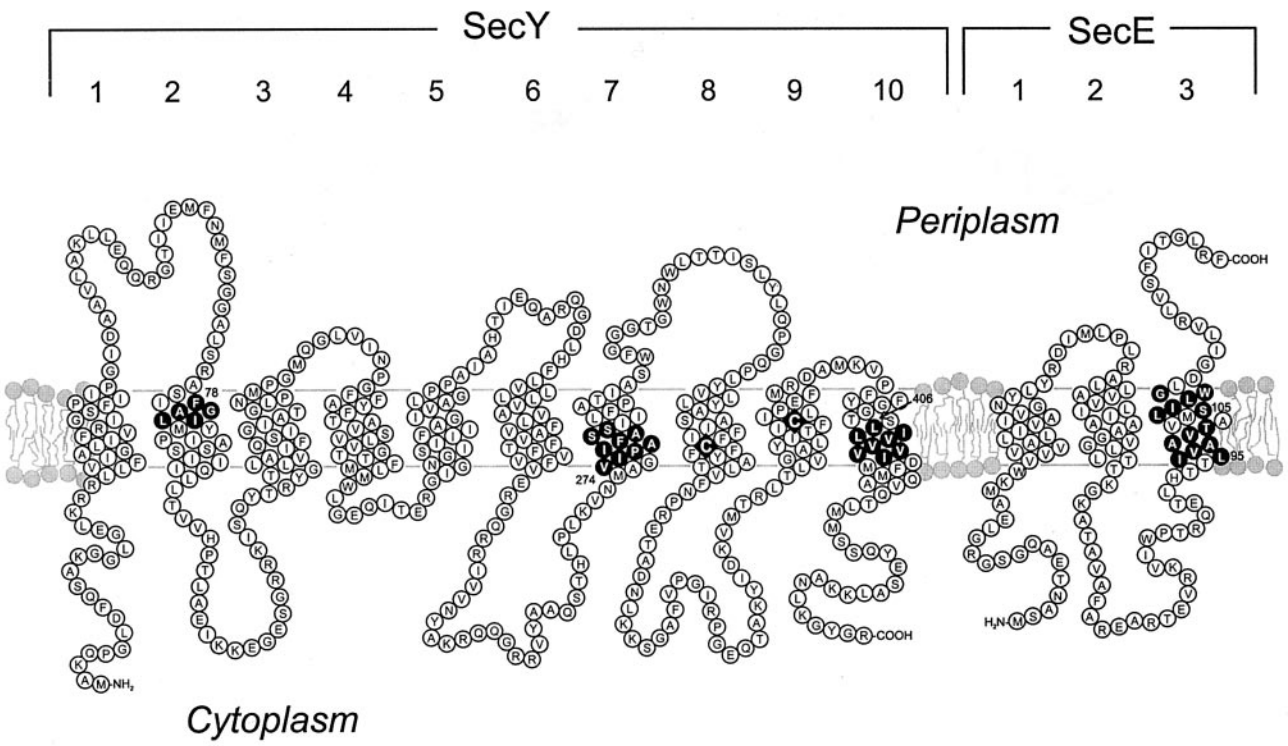


FIG. 1. **Membrane topology of *E. coli* SecY and SecE.** The *black diamonds* represent endogenous cysteine residues in SecY that were replaced by serine residues. The residues that were replaced by cysteine are depicted as *black circles*.

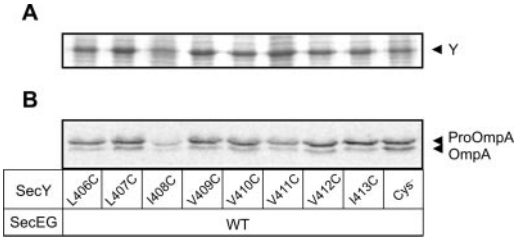


FIG. 2. **Expression levels and activities of SecYEG complexes harboring a cysteine mutation in TMS 10 of SecY.** IMVs containing overexpressed SecYEG mutants were analyzed by: *A,* a Coomassie Brilliant Blue stained gel showing the levels of His-tagged SecY overexpression. *B, in vitro* translocation of proOmpA. SecY, proOmpA, and OmpA are indicated by *arrows*.

combinations in TMS 10 of SecY (at positions 406–413) and TMS 3 of SecE (at positions 95–101). The overexpression level and activity of the SecYEG complexes, which contain the SecE cysteine mutations that are used in this study, have been analyzed before and shown to be similar to wild-type SecYEG (18). SecYEG IMVs of 49 pairs of cysteine mutations exhibited normal levels of overexpression whereas the 7 combinations with SecY I408C showed a lower SecY expression level (data not shown). IMVs, corrected for the SecY level, were oxidized with 1 mM $Cu^{2+}$(phenanthroline)$_3$ and analyzed by SDS-PAGE and immunoblotting using antibodies against SecY and SecE (Fig. 3). Four cysteine combinations display reproducibly a higher molecular mass band, which reacts with both antibodies against SecY and SecE and corresponds to an expected SecY-SecE cross-link. In particular the combinations SecY(V409C)-SecE(T101C) and SecY(I413C)-SecE(V100C) yielded a strong SecY-SecE cross-link. As shown previously for other identified cross-links (18), oxidation of these cysteine mutant pairs resulted in the inactivation of the protein translocation reaction, whereas the activity was recovered after reduction with dithiothreitol (data not shown). Several other cysteine pairs, especially in combination with SecY I408C, show a faint band at the position of the expected SecY-SecE cross-link (Fig. 3). These bands are significantly weaker than those for the four cysteine pairs mentioned above, did not stain with the SecE antibody, and lacked apparent reproducibility. Therefore, we do not believe that these bands reflect clear contact points between SecY and SecE. The cross-linking data could be modeled by assuming an $\alpha$-helical contact interface between TMS 10 of SecY and TMS 3 of SecE (Figs. 4 and 5).

*Model for the Core of the SecYE Complex*—To incorporate the identified cross-links into a three-dimensional model, TMS 2 ($Ala^{75}$–$Ile^{92}$), 7 ($Val^{274}$–$Ala^{291}$), and 10 ($Val^{397}$–$Met^{414}$) of SecY and TMS 3 ($Leu^{95}$–$Asp^{112}$) of SecE were built as $\alpha$-helices *in silico.* Strikingly, TMS 7 and 10 of SecY contact the same side of TMS 3 of SecE. However, the position on SecE ($Val^{97}$) that shows the strongest cross-linking reaction with TMS 7 of SecY is located at a different depth in the membrane than the positions ($Val^{100}$ and $Thr^{101}$) that are the strongest contact sites to TMS 10 of SecY. Only one model (Fig. 5) could explain all 13 observed transmembrane contacts (Refs. 17 and 18 and this study). Remarkably, this model implies a strongly tilted SecE helix surrounded by TMS 2, 7, and 10 of SecY. We therefore conclude that TMS 3 of SecE is tilted relative to the surrounding transmembrane segments of SecY in the core of the translocase.

## DISCUSSION

To fully understand the mechanism of translocation and membrane insertion of proteins, detailed structural information of the translocase is essential. The highest level of structural information can be derived from x-ray crystallography. However, crystallization of membrane proteins is very difficult to accomplish. This is in particular a major challenge with the SecYEG complex as it needs to interact with the soluble SecA protein to form a functional translocase. Recently, two-dimensional crystals of SecYEG have been produced from which a 9-Å projection structure was calculated, but the structural information in this projection of SecYEG is limited as it is not

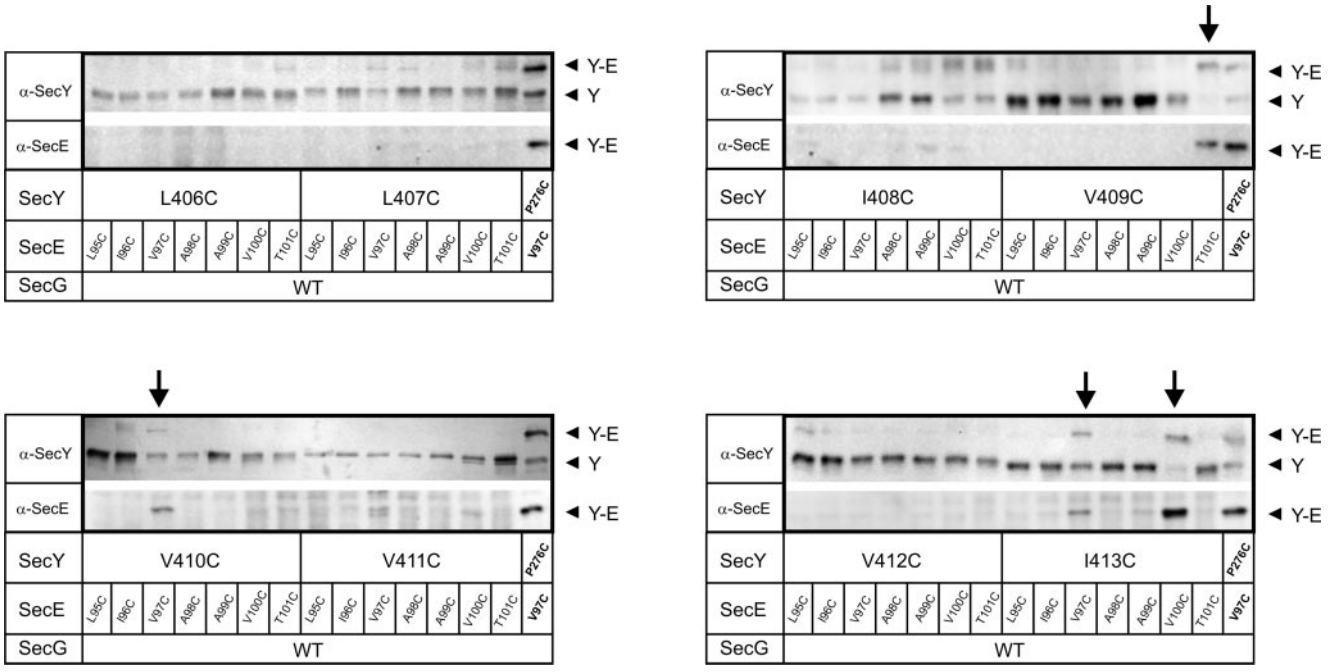


FIG. 3. **Identification of the sites of contact between TMS 10 of SecY and TMS 3 of SecE.** Eight consecutive unique cysteine mutations in SecY TMS 10 were co-expressed with seven cysteine mutations in SecE TMS 3 and wild-type SecG. IMVs containing the mutant SecYEG complexes were oxidized with 1 mM $Cu^{2+}$(phenanthroline)$_3$ and analyzed by 12% SDS-PAGE and immunoblotting using antibodies against SecY and SecE. Mutant SecY(P276C)E(V97C)G that gives a cross-link between TMS 7 of SecY and TMS 3 of SecE was included as a control (18). The bands representing SecY (*Y*) and SecY-SecE cross-link (*Y-E*) (50 kDa) are indicated by *arrows*.

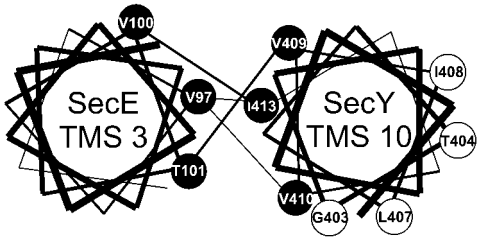


FIG. 4. **Schematic representation of the contact interface between TMS 10 of SecY and TMS 3 of SecE.** Schematic top view of TMS 10 of SecY and TMS 3 of SecE, which are depicted as helices. Cysteine-substituted residues involved in SecY-SecE cross-linking are shown as *closed circles* and connected by a *line*. Sites of known *prlA* mutations are displayed as *open circles*.

possible to assign the helices at this resolution (21). An alternative approach for obtaining structural information is cysteine-scanning mutagenesis, a technique that can be used to map the sites of contact between the transmembrane segments in membrane proteins. An important advantage of this technique is that structural information is obtained from the functional, membrane-embedded proteins, and observed sites of interaction can be further exploited to obtain information on the dynamics of the proteins involved. We have used this technique to reveal the sites of interaction between SecY and SecE, both essential components of the protein-conducting channel. In this study, we show that TMS 3 of SecE contacts TMS 10 of SecY. Furthermore, we present a three-dimensional model of the SecYE core based on the combined cross-linking data.

We have identified multiple sites of contact between SecY and SecE and between two neighboring SecE molecules. Using pairs of cysteine mutations, sites of contact were identified between TMS 3 of SecE and TMS 2 (S105C-I82C; L108C-F78C; L108C-A79C) (17) and TMS 7 (V97C-P276C; V100C-A280C; T101C-A280C) (18) of SecY. Here, we show that TMS 3 of SecE also contacts TMS 10 of SecY (V97C-V410C; V97C-I413C; V100C-I413C; T101C-V409C) (Fig. 3). All cross-links reappear periodically, consistent with an $\alpha$-helical structure of these transmembrane segments (Figs. 4 and 5*A*). Oligomeric forms of SecYEG were revealed by covalently linked SecE dimers when cysteines are introduced at the positions of $Ala^{99}$, $Leu^{106}$, and $Gly^{110}$ in TMS 3 (17, 18). These contacts also display spatial periodicity, indicating an $\alpha$-helical interface that covers the entire span of the membrane. Furthermore, the SecE dimer interface is mapped opposite to the SecY-SecE contacts (Fig. 5*B*).

*prl* mutations in SecY and SecE result in thermally induced destabilization of the SecY-SecE interaction (30). The current study shows that the positions of known *prlA* mutations in TMS 10 are directed away from the SecY-SecE interface (Fig. 4). This phenomenon has also been observed previously for TMS 2 and 7 of SecY (18). This implies that the effect on the SecY-SecE interaction caused by *prl* mutations must be indirect, probably mediated by a local disturbance of the structure or helical packing. The mutation I408C in SecY resulted in lowered expression levels, but the translocation activity was found to be comparable with cysteine-less SecYEG when corrected for the reduced SecY levels (Fig. 2). $Ile^{408}$ is a hot spot for known *prl* mutations and thus sensitive to mutational changes. However, I408C did not yield a strong *prl* phenotype as assayed by translocation of Δ8-proOmpA (data not shown).

Strikingly, the suggested contact interfaces of TMS 3 of SecE to TMS 7 and 10 of SecY are overlapping. An effort to fit all observed inner membrane cross-links resulted in the model shown in Fig. 5. For this, TMS 2, 7, and 10 of SecY and TMS 3 of SecE were modeled as $\alpha$-helices and arranged such that all identified sites of contact could be accommodated. Extensive modeling and probing of the different contacts resulted in only one model that met the set criteria. Other models could not fit the complete set of identified cross-links or even generate expected sites of contact that were not observed experimentally. Our model revealed a tilted TMS 3 of SecE relative to the surrounding TMS 2, 7, and 10 of SecY. Furthermore, a tilted helix implies a crossed contact interface between two SecYE

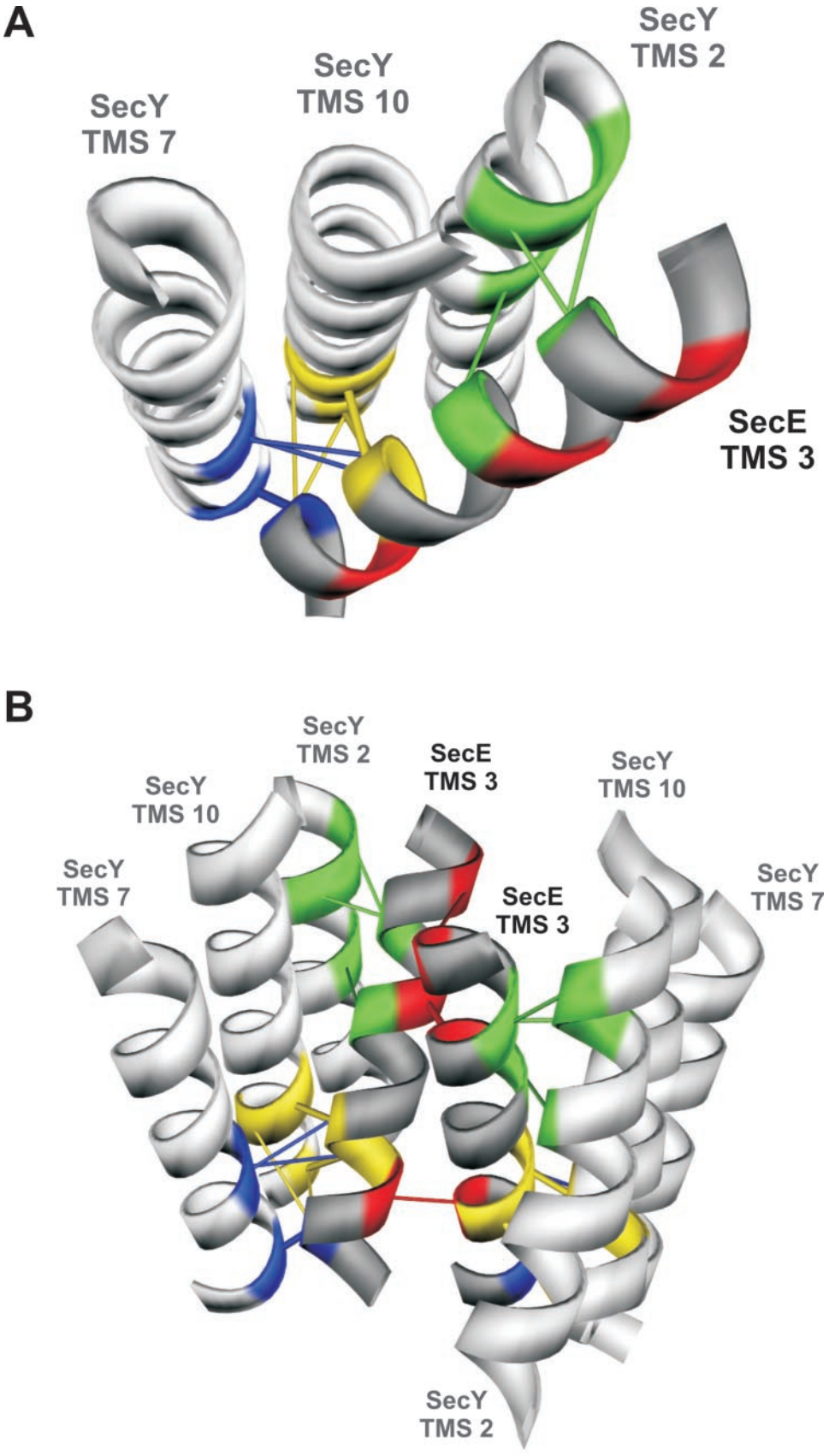


FIG. 5. **Three-dimensional models of the SecYE complex.** Side view of helices representing TMS 2, 7, and 10 of SecY and TMS 3 of SecE. *A,* monomeric view; *B*, dimeric view. SecY and SecE helices are indicated and displayed in *white* and *gray*, respectively. *Colored patches* and *lines* are used to specify the residues that are involved in contacts between TMS 3 of SecE and the following helices of SecY: TMS 2 (*green*), TMS 7 (*blue*), and TMS 10 (*yellow*). TMS 7 and 10 of SecY can be cross-linked to the same residues of SecE. Therefore, the residues involved are colored only according to their strongest contacts (*i.e.* SecE $Val^{97}$ in *blue*; $Val^{100}$ and $Thr^{101}$ in *yellow*). Sites of contact between neighboring SecE molecules are depicted in *red patches* and connected by *red lines*. Efficiency of cross-linking is categorized in strong (*thick lines*) and weak (*thin lines*).

molecules and the presence of an optimal point of contact because the formation of a SecYE dimer involves TMS 3 of SecE (Fig. 5*B*). Indeed, $Leu^{106}$ of SecE has been observed as an optimal point of contact as the SecE-SecE cross-linking efficiency for the L106C mutation is significantly higher than for the surrounding A99C and G110C (18). We believe that our model is a correct representation of the core of the translocase because: 1) it accommodates all 13 identified inner membrane contacts; 2) periodically re-appearing contacts have been found for every helix-helix interface; and 3) it predicts no additional strong cross-links other than those already observed for the cysteine combinations we have tested. Strikingly, a recent three-dimensional reconstruction of the SecYEG dimer from two-dimensional crystals reveals the presence of two highly tilted helices at the SecYEG contact interface (31). Because SecE has been mapped at this interface, we propose that these helices represent the SecE dimer contact interface (17, 18).

The dynamics of the identified interactions within the functional translocase have been investigated before (17, 18). The formation of thiol-stabilized interactions in the interface between TMS 3 of SecE and TMS 7 of SecY and another TMS 3 of SecE inhibits preprotein translocation reversibly (17, 18). This is also observed for the identified SecY TMS 10–SecE TMS 3 contacts (data not shown). These disulfide bonds can, however, also be formed between SecY and SecE (17, 18) and even much more efficiently between neighboring SecE molecules (17) during an active cycle of preprotein translocation. Therefore, transient flexibility and conformational changes within the integral membrane domain of the translocase appear essential for its function. The current data will facilitate future attempts to resolve the structure of the translocase and to study its dynamic nature during preprotein translocation.

*Acknowledgments*—We would like to thank Jeanine de Keyzer and Jelto Swaving for their help and fruitful discussions and Eli van der Sluis for critically reviewing the manuscript.

REFERENCES

1. Driessen, A. J. M., Manting, E. H., and van der Does, C. (2001) *Nat. Struct. Biol.* **8,** 492–498
2. Mori, H., and Ito, K. (2001) *Trends Microbiol.* **9,** 494–500
3. Brundage, L., Hendrick, J. P., Schiebel, E., Driessen, A. J. M., and Wickner, W. T. (1990) *Cell* **62,** 649–657
4. Hanada, M., Nishiyama, K. I., Mizushima, S., and Tokuda, H. (1994) *J. Biol. Chem.* **269,** 23625–23631
5. Hartl, F. U., Lecker, S., Schiebel, E., Hendrick, J. P., and Wickner, W. T. (1990) *Cell* **63,** 269–279
6. Schiebel, E., Driessen, A. J. M., Hartl, F. U., and Wickner, W. T. (1991) *Cell* **64,** 927–939
7. Economou, A., and Wickner, W. T. (1994) *Cell* **78,** 835–843
8. van der Wolk, J. P., de Wit, J. G., and Driessen, A. J. M. (1997) *EMBO J.* **16,** 7297–7304
9. Pogliano, J. A., and Beckwith, J. (1994) *EMBO J.* **13,** 554–561
10. Schatz, P. J., Bieker, K. L., Ottemann, K. M., Silhavy, T. J., and Beckwith, J. (1991) *EMBO J.* **10,** 1749–1757
11. Joly, J. C., Leonard, M. R., and Wickner, W. T. (1994) *Proc. Natl. Acad. Sci. U. S. A.* **91,** 4703–4707
12. Kihara, A., Akiyama, Y., and Ito, K. (1995) *Proc. Natl. Acad. Sci. U. S. A.* **92,** 4532–4536
13. Baba, T., Taura, T., Shimoike, T., Akiyama, Y., Yoshihisa, T., and Ito, K. (1994) *Proc. Natl. Acad. Sci. U. S. A.* **91,** 4539–4543
14. Pohlschroder, M., Murphy, C., and Beckwith, J. (1996) *J. Biol. Chem.* **271,** 19908–19914
15. Flower, A. M., Osborne, R. S., and Silhavy, T. J. (1995) *EMBO J.* **14,** 884–893
16. Harris, C. R., and Silhavy, T. J. (1999) *J. Bacteriol.* **181,** 3438–3444
17. Kaufmann, A., Manting, E. H., Veenendaal, A. K. J., Driessen, A. J. M., and van der Does, C. (1999) *Biochemistry* **38,** 9115–9125
18. Veenendaal, A. K. J., van der Does, C., and Driessen, A. J. M. (2001) *J. Biol. Chem.* **276,** 32559–32566
19. Plath, K., Mothes, W., Wilkinson, B. M., Stirling, C. J., and Rapoport, T. A. (1998) *Cell* **94,** 795–807
20. Manting, E. H., van der Does, C., Remigy, H., Engel, A., and Driessen, A. J. M. (2000) *EMBO J.* **19,** 852–861
21. Collinson, I., Breyton, C., Duong, F., Tziatzios, C., Schubert, D., Or, E., Rapoport, T., and Kuhlbrandt, W. (2001) *EMBO J.* **20,** 2462–2471
22. Bessonneau, P., Besson, V., Collinson, I., and Duong, F. (2002) *EMBO J.* **21,** 995–1003
23. Yahr, T. L., and Wickner, W. T. (2000) *EMBO J.* **19,** 4393–4401
24. Cabelli, R. J., Chen, L., Tai, P. C., and Oliver, D. B. (1988) *Cell* **55,** 683–692
25. Weiss, J. B., Ray, P. H., and Bassford, P. J., Jr. (1988) *Proc. Natl. Acad. Sci. U. S. A.* **85,** 8978–8982
26. Crooke, E., Guthrie, B., Lecker, S., Lill, R., and Wickner, W. T. (1988) *Cell* **54,** 1003–1011
27. van der Does, C., Manting, E. H., Kaufmann, A., Lutz, M., and Driessen, A. J. M. (1998) *Biochemistry* **37,** 201–210
28. van der Wolk, J. P., Fekkes, P., Boorsma, A., Huie, J. L., Silhavy, T. J., and Driessen, A. J. M. (1998) *EMBO J.* **17,** 3631–3639
29. de Keyzer, J., van der Does, C., Swaving, J., and Driessen, A. J. M. (2002) *FEBS Lett.* **510,** 17–21
30. Duong, F., and Wickner, W. T. (1999) *EMBO J.* **18,** 3263–3270
31. Breyton, C., Haase, W., Rapoport, T. A., Kuhlbrandt, W., and Collinson, I. (2002) *Nature* **418,** 662–665